Spontaneous relapsing-remitting EAE in the SJL/J mouse: MOG-reactive transgenic T cells recruit endogenous MOG-specific B cells

Bernadette Pöllinger,[1] Gurumoorthy Krishnamoorthy,[1] Kerstin Berer,[1] Hans Lassmann,[3] Michael R. Bösl,[2] Robert Dunn,[4] Helena S. Domingues,[1] Andreas Holz,[1] Florian C. Kurschus,[1] and Hartmut Wekerle[1]

[1]Department of Neuroimmunology and [2]Transgenic Service, Max Planck Institute of Neurobiology, D-82152 Martinsried, Germany
[3]Center for Brain Research, Medical University of Vienna, A-1090 Vienna, Austria
[4]Department of Immunology, Biogen Idec, San Diego, CA 92122

We describe new T cell receptor (TCR) transgenic mice (relapsing-remitting [RR] mice) carrying a TCR specific for myelin oligodendrocyte glycoprotein (MOG) peptide 92–106 in the context of I-A^s. Backcrossed to the SJL/J background, most RR mice spontaneously develop RR experimental autoimmune encephalomyelitis (EAE) with episodes often altering between different central nervous system tissues like the cerebellum, optic nerve, and spinal cord. Development of spontaneous EAE depends on the presence of an intact B cell compartment and on the expression of MOG autoantigen. There is no spontaneous EAE development in B cell–depleted mice or in transgenic mice lacking MOG. Transgenic T cells seem to expand MOG autoreactive B cells from the endogenous repertoire. The expanded autoreactive B cells produce autoantibodies binding to a conformational epitope on the native MOG protein while ignoring the T cell target peptide. The secreted autoantibodies are pathogenic, enhancing demyelinating EAE episodes. RR mice constitute the first spontaneous animal model for the most common form of multiple sclerosis (MS), RR MS.

CORRESPONDENCE
Hartmut Wekerle:
hwekerle@neuro.mpg.de
OR
Florian C. Kurschus:
kurschus@neuro.mpg.de

Abbreviations used: cDNA, complementary DNA; CNS, central nervous system; EAE, experimental autoimmune encephalomyelitis; MOG, myelin oligodendrocyte glycoprotein; MS, multiple sclerosis; NTL, nontransgenic littermate; OSE, opticospinal EAE; OSMS, opticospinal MS; PI, propidium iodide; rMOG, recombinant rat MOG; RR, relapsing-remitting.

Autoimmune diseases can affect most organs of the body including liver, heart, the endocrine system, the musculoskeletal apparatus, and the central nervous system (CNS). They commonly start off at a young age and then last throughout life, often resulting in severe disability. The factors that trigger the onset, modulate the course, and determine the clinical character of autoimmune diseases have remained obscure, a deficit of knowledge which sets limits to the design of specific and efficient therapies.

Yet there is increasing evidence that organ-specific autoimmune diseases, such as rheumatoid arthritis, type 1 diabetes mellitus, and multiple sclerosis (MS), are the result of a pathogenic interaction of autoimmune T and B cells. There is substantial information on the role of T cells in organ-specific autoimmunity. Some act as effector cells attacking self-tissues, either directly or via recruiting accessory cells like macrophages. Other T cells regulate the time course of the response and still others provide help to autoantibody-producing B cells. The contribution of autoimmune B cells to the inflammatory pathogenesis seems to be complex as well. Beyond producing humoral autoantibodies, B cells serve as APCs activating pathogenic T cells, and, through their capacity of releasing cytokines, B cells are involved in shaping local microenvironments favorable to evolving cellular autoimmune responses.

A. Holz's present address is Department of Cellular and Molecular Biology, Technical University of Braunschweig, D-38106 Braunschweig, Germany.
B. Pllinger's present address is Novartis Pharma AG, CH-4056 Basel, Switzerland.
F.C. Kurschus's present address is I. Medizinische Klinik und Poliklinik, Johannes Gutenberg Universität, D-55131 Mainz, Germany.

The Rockefeller University Press $30.00
J. Exp. Med. Vol. 206 No. 6 1303-1316
www.jem.org/cgi/doi/10.1084/jem.20090299

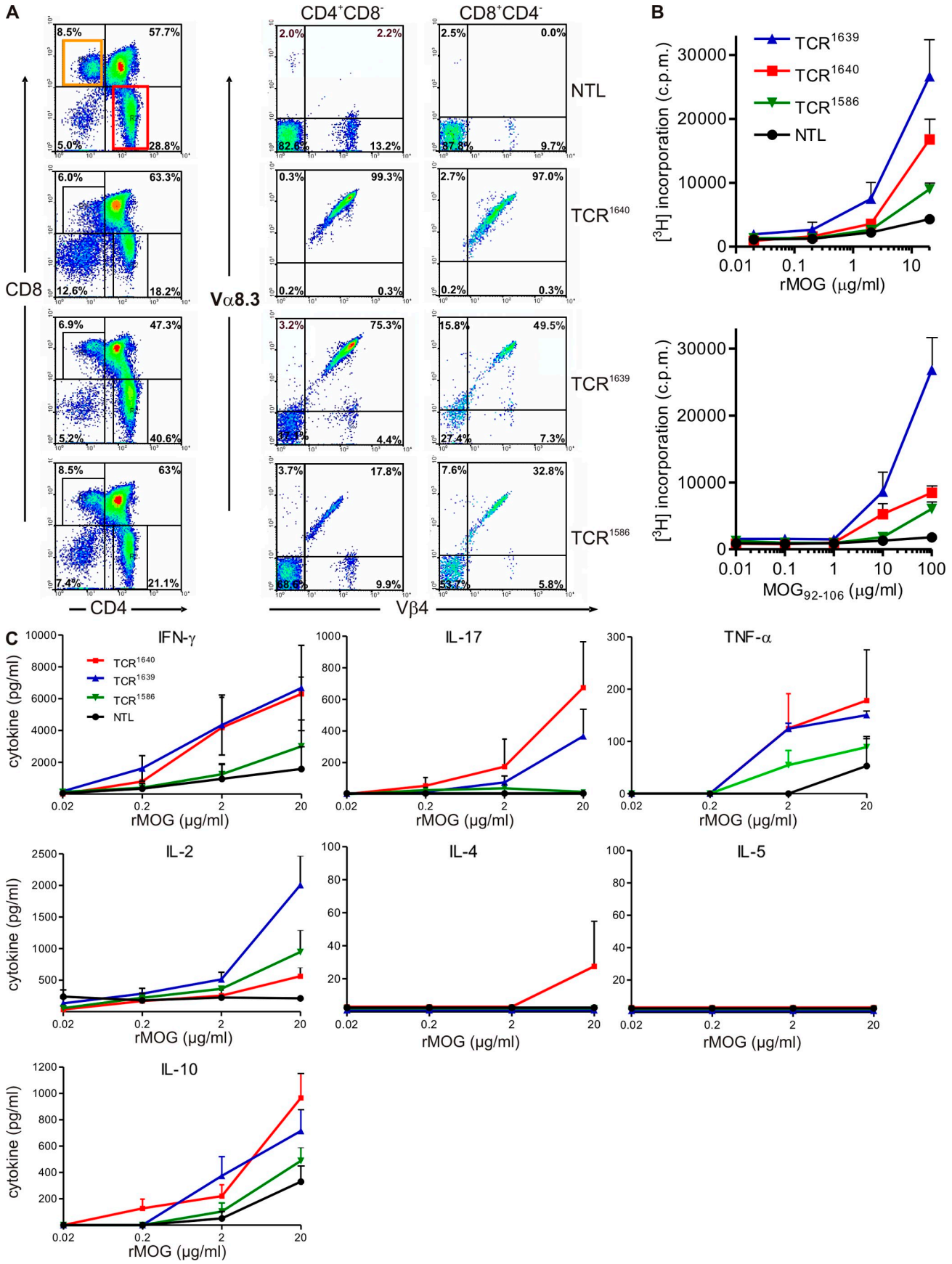

Deciphering the interactions between T and B cells in the spontaneous development of organ-specific autoimmune responses requires suitable animal models. Naturally occurring models are available for type 1 diabetes mellitus and systemic lupus erythematosus but not for autoimmunity in the CNS (1). Recently, we and others described a double-transgenic mouse model, which simulates opticospinal MS (OSMS) remarkably well, a variant of which is also known as Devic's disease (2, 3). These mice, termed opticospinal experimental autoimmune encephalomyelitis (EAE [OSE]) mice, express myelin oligodendrocyte glycoprotein (MOG)–specific receptors on T and B cells and spontaneously develop demyelinating inflammatory disease at frequencies >50%. Like in human OSMS (4), the lesions in affected mice are restricted to optic nerve and spinal cord, and, in most cases, the disease takes a chronic progressive course without remissions and marked relapses. It should, however, be noted that the type of MS that most prevalently affects Caucasian populations differs fundamentally from OSMS (5). Typically, MS starts out with a relapsing-remitting (RR) course, where disease episodes may completely resolve only to be followed by a subsequent relapse. In this disease variant, the pathogenic lesions, demyelinating plaques, may be located throughout the CNS, thus causing the notoriously varied neurological defect patterns.

In this paper, we describe a new transgenic mouse model that spontaneously develops RR-EAE and, thus, recapitulates the "Western" variant of MS. Furthermore, and most importantly, we found that in these mice transgenic autoimmune T cells expand autoimmune B cells from the endogenous immune repertoire and guide them to produce antibodies against conformational epitopes of the MOG protein, which, together with complement, may initiate the destruction of MOG-expressing target cells.

RESULTS

New MOG-specific TCR transgenic SJL/J mice

We generated transgenic mice expressing a TCR specific for the rat/mouse MOG peptide 92–106 in the context of I-A^s. This TCR, which uses Vα8.3 and Vβ4 genes, was derived from a MOG-specific encephalitogenic Th1-$CD4^+$ T cell clone isolated from a WT SJL/J mouse immunized against recombinant rat MOG (rMOG; Fig. S1). We selected three founder lines differing in markedly distinct proportions of transgenic $V\alpha8.3^+/V\beta4^+$ $CD4^+$ T cells in central and peripheral immune repertoires (Fig. 1 A and Fig. S2). In low frequency TCR^{1586} mice, 18% of single-positive $CD4^+CD8^-$ thymocytes expressed the transgenic TCR. The proportion was 75% in medium frequency TCR^{1639} mice and 99% in high frequency TCR^{1640} mice (Fig. 1 A). In all three transgenic mouse lines, transgene expression levels in the peripheral immune system were proportional to the ones in the central thymic repertoires (Fig. S2).

The density of the transgenic TCR on the surface of mature $CD4^+$ T cells in the spleen varied markedly (Fig. S2). Especially in high frequency TCR^{1640} spleens, T cells could be distinguished based on the low and high densities of surface TCR (dim and bright TCR). The dim TCR population expressed higher levels of CD25 and CD69 and lower levels of CD62L (unpublished data).

Stimulation of nonimmunized transgenic spleen cells with rMOG or $MOG_{92\text{-}106}$ peptide in vitro led to dose-dependent proliferative responses (Fig. 1 B). Concomitant cytokine responses largely followed the proliferation pattern. Although the secretion of proinflammatory IFN-γ, IL-17, and antiinflammatory IL-10 was similar in TCR^{1640} and TCR^{1639} lines, IL-2 secretion was higher in TCR^{1639} T cells. The Th2-related cytokines IL-4 and IL-5 were absent in nearly all samples tested (Fig. 1 C).

Spontaneous EAE in single- and double-transgenic SJL/J anti-MOG mice: RR course with varied clinical syndromes

While continuously backcrossing the line TCR^{1640} into the SJL/J background, we noted spontaneous EAE-like disease developing at a high frequency (Fig. 2 A and Table S1). In the eighth backcross generation, >80% of all females developed EAE within 160 d. During the same period, the EAE rate in males was >60%. EAE was rare in transgenic SJL/J mice with low frequency TCR^{1586} and surprisingly absent in medium frequency TCR^{1639} mice and in *Mog*-deficient TCR^{1640} ($TCR^{1640} \times Mog^{-/-}$) mice (Table S1).

We and others previously described a double-transgenic mouse strain, OSE mice (2, 3), which expressed a MOG-specific TCR transgene, 2D2 (specific for MOG peptide 35–55 in context of I-A^b), along with the gene coding for the rearranged IgH variable chain of the classical anti-MOG monoclonal antibody, 8.18-C5 (IgH^{MOG} mice) (6). We have now created similar double-transgenic mice by mating TCR^{1640} SJL/J mice to IgH^{MOG} on SJL/J background. Double-transgenic $TCR^{1640} \times IgH^{MOG}$ mice developed spontaneous EAE very similar to TCR^{1640} single transgenics, with some apparently minor differences. Almost all double-transgenic females came down with disease by 120 d of age, whereas males of the same age showed an EAE rate of <40%. This gender gap was highly significant but narrowed during the subsequent weeks (Fig. 2 A).

Figure 1. Characterization of a new MOG-specific TCR transgenic SJL/J mouse. (A) Thymocytes from 8–10-wk-old TCR transgenic mice or NTLs were stained with antibodies to CD4, CD8, TCR-Vβ4, and TCR-Vα8.3 and cells were analyzed by flow cytometry. Representative figures of three to seven analyzed mice are shown. Transgenic Vα8.3 and Vβ4 are shown on cells gated as indicated, either $CD4^+/CD8^-$ or $CD4^-/CD8^+$. (B) Proliferative response to recombinant MOG protein (rMOG) or MOG peptide 92–106 measured as ^{3}H-thymidine incorporation. Splenocytes from TCR transgenic mice (8–10-wk-old healthy) were cultured with indicated concentrations of rMOG (top) and $MOG_{92\text{-}106}$ (bottom). (C) Cytokine responses to rMOG. Indicated cytokines were measured in supernatants harvested 48 h after rMOG activation by ELISA. Pooled data from three independent experiments are shown. Error bars indicate SEM. B and C: TCR^{1640}, $n = 3$; TCR^{1639}, $n = 3$; TCR^{1586}, $n = 3$; NTL, $n = 2$.

Table I. Spontaneous EAE in TCR transgenic SJL/J mice: course of disease

Mice (gender)	RR (n)		Progressive (n)
	With full remission	With partial remission	
	%	%	%
TCR^{1640} (f)	71.4 (5/7)	14.3 (1/7)	14.3 (1/7)
TCR^{1640} (m)	35.3 (6/17)	11.7 (2/17)	53 (9/17)
TCR^{1640} × IgH^{MOG} (f)	43.7 (7/16)	25.0 (4/16)	31.2 (5/16)
TCR^{1640} × IgH^{MOG} (m)	6.2 (1/16)	25.0 (4/16)	68.8 (11/16)
rMOG imm. SJL/J (f)	10.0 (1/10)	70.0 (7/10)	20 (2/10)

f, female; m, male; imm., immunized.

We also crossed IgH^{MOG} mice to the medium and low frequency lines TCR^{1639} and TCR^{1586}, respectively. Only 1 out of 17 medium frequency TCR^{1639} × IgH^{MOG} mice displayed EAE and none of the low frequency TCR^{1586} × IgH^{MOG} showed any clinical symptoms (Table S1).

The CNS disease spontaneously developing in TCR transgenic SJL/J mice differed dramatically from spontaneous OSE seen in OSE mice (2, 3). In TCR transgenic SJL/J mice, single-transgenic TCR^{1640} mice, and double-transgenic TCR^{1640} × IgH^{MOG} mice, disease was extremely variable both in course and

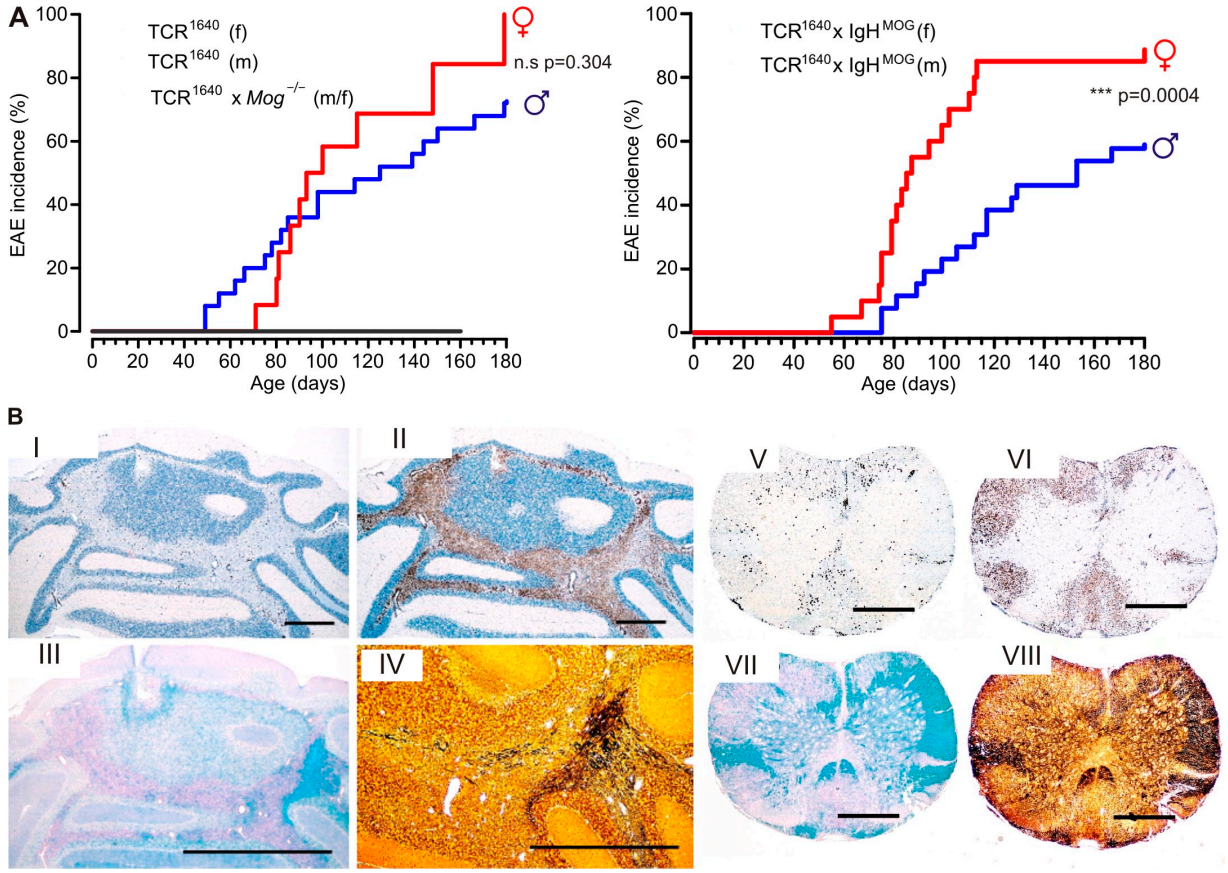

Figure 2. Spontaneous RR-EAE in TCR transgenic SJL/J mice. (A) Male and female single-transgenic TCR^{1640} compared with double-transgenic TCR^{1640} × IgH^{MOG} mice. Shown is the spontaneous incidence of first signs of ataxia or classical EAE-like symptoms in TCR^{1640} (left) and double-transgenic TCR^{1640} × IgH^{MOG} (right) mice. TCR^{1640} females (f), $n = 12$; males (m), $n = 27$; TCR^{1640} × IgH^{MOG} females, $n = 20$; males, $n = 26$; TCR^{1640} × $Mog^{-/-}$ mice, $n = 6$. Disease kinetic of genders in TCR^{1640} mice was not statistically significant (P = 0.304) but differed significantly between sexes of TCR^{1640} × IgH^{MOG} mice (P = 0.0004). (B) Histological analysis of cerebellum and spinal cord from a sick TCR^{1640} mouse (RR mouse) with ataxia and classical paralysis. Cerebellum (I–IV) and spinal cord (V–VIII) showed severe infiltration, demyelination, and axonal damage as visualized by immunohistochemistry using anti-CD3 (I and V) and anti–Mac3 antibodies (II and VI), Luxol fast blue staining (III and VII), and Bielschowsky silver impregnation (IV and VIII). I, II, V, and VI were counterstained by hematoxylin and eosin (H&E). Magnification: ×17 (cerebellum) and ×30 (spinal cord). Bars, 1 mm. Data are representative of at least two independent experiments consisting of more than three mice per group.

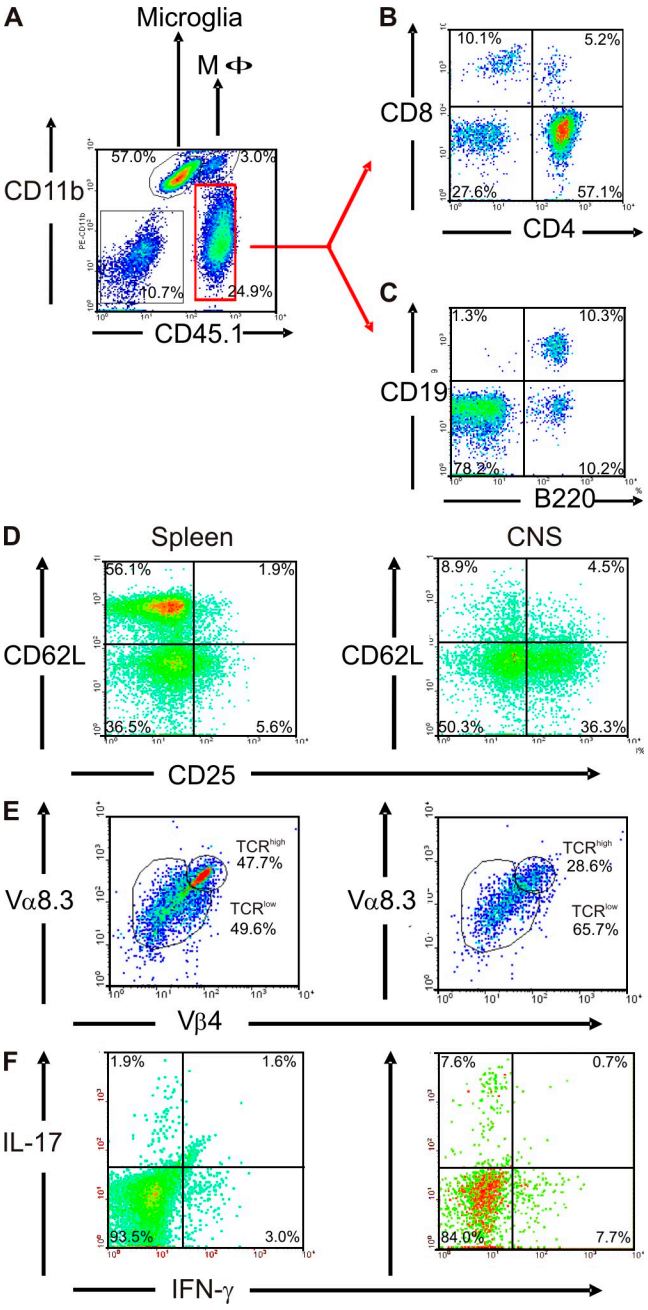

Figure 3. Inflammatory cell infiltrates in RR-EAE lesions. (A–C) Cellular infiltrate into the CNS of sick TCR^{1640} mice (score 3) is composed of macrophages, T cells, and B cells. CNS mononuclear cells were isolated from a sick TCR^{1640} mouse and stained against CD11b and CD45.1 (A), together with CD8 and CD4 (B) or together with CD19 and B220 (C). Cells in B and C were analyzed among gated CD45.1$^+$CD11b$^-$ cells (red region as indicated). (D–F) Activation and Th1/Th17 cytokine expression of infiltrating CD4$^+$ T cells. (D) CNS infiltrate cells express CD25, but not CD62L, and partially down-modulate their TCR (Vα8.3 and Vβ4). Activation status and TCR expression was compared between splenocytes (left) and CNS-isolated cells (right). (E) CD4$^+$CD3$^+$ T cells infiltrating the CNS of sick TCR^{1640} mice predominantly expressed the pathogenic TCR composed of Vα8.3 and Vβ4 chains in a low expression level (TCR^{low}) compared with the spleen. Numbers indicate the percentage of stained cells in the respective quadrant or region. (F) Intracellular cytokine staining after stimulation with PMA/ionomycin in brefeldin A. Th1 (IFN-γ$^+$/IL-17$^-$) and Th17 (IFN-γ$^-$/IL-17$^+$) cells are enriched in CNS infiltrates of sick TCR^{1640} (score 3.5) mice compared with splenocytes. D–F were analyzed among gated CD45.1$^+$CD4$^+$ cells. Flow cytometry data are representative of three to five sick TCR^{1640} mice analyzed in three to five independent experiments.

clinical nature. Typically, in females EAE started with an RR course. Often, the first attacks resolved completely but were followed by further bouts. Intriguingly, individual EAE bouts often differed radically in their neurological defects. In a substantial number of cases, the initial bout was dominated by ataxia rather than by classical EAE defects. Affected mice were unable to walk along a straight line, deviating and falling to the side, but did not show limb weakness or paralysis (Video 1). In many cases, the mice recovered completely until a first relapse, which commonly showed a completely different clinical picture, for example, hind limb paralysis as seen in typical EAE. Again, this second disease episode subsided, giving way to partial remission. Later disease episodes mostly showed classical paralytic EAE (Table I and Fig. S3).

Although there was no clear distinction between single- and double-transgenic SJL/J mice, EAE course differed between females and males. As detailed in Table I, RR disease was more common in females. A minority of female mice developed progressive EAE from the beginning, but more than half of the males developed primary progressive EAE.

CNS changes representing different clinical EAE episodes

The clinical deficiencies developing in affected mice were reflected by the location and character of underlying CNS lesions. Ataxic mice displayed large inflammatory and demyelinated lesions in cerebellum and brain stem (Fig. 2 B). In contrast, in mice suffering from conventional EAE, lesions were distributed throughout the spinal cord, brain stem, and optic nerve (Table S2).

Irrespective of their location within the CNS, the inflammatory lesions were characterized by numerous CD3$^+$ T cells in the middle of a plethora of Mac3-positive activated macrophage-like cells (Fig. 2 B). The inflammatory infiltrates were embedded in large areas of demyelination and axon destruction. In line with their comparable clinical score, the histological patterns were similar between TCR^{1640} single-transgenic and TCR^{1640} × IgH^{MOG} double-transgenic mice (Table S2).

Cytofluorimetric analyses confirmed that, within the CNS, the major infiltrating inflammatory lymphocytes were CD4$^+$ T cells and B cells together with a minor population of macrophages and CD8$^+$ T cells (Fig. 3, A–C), with only minor contributions from CD8$^+$ T cells. Notably, most transgenic CD4$^+$ T cells infiltrating the CNS were activated. Many cells expressed the activation marker CD25 and were CD62L negative (Fig. 3 D). Additionally, infiltrating CD4$^+$ T cells expressed the activation markers CD44, VLA4, and ICOS (unpublished data). Furthermore, a high proportion (>65%) of CNS-infiltrating transgenic T cells partly down-modulated

their transgenic Vβ4 and Vα8.3 determinants, which is in contrast to peripheral splenic populations, where the modulated subpopulations comprised less than half of the entire transgenic $CD4^+$ T cell subset (Fig. 3 E).

In agreement with previous EAE studies (7–10), we found CNS-infiltrating Th1 (IFN-γ^+/IL-17^-) and Th17 (IFN-γ^-/IL-17^+) cells. Compared with spleen, Th17 cells were enriched in CNS threefold and Th1 cells more than twofold (Fig. 3 F). A substantial part of the activated $CD4^+CD25^+$ infiltrate T cells express transcription factor Foxp3, a marker of regulatory T cells (not depicted) (11).

Next, we measured the cytokine milieu in brain and spinal cord of TCR^{1640} mice in different disease stages by real-time PCR in comparison to rMOG immunized SJL/J mice (Fig. S4). Most cytokines followed an infiltration pattern proportional to CD4 expression. As expected from our infiltrate analysis (Fig. 3), we found expression of both IFN-γ and IL-17 in diseased mice. In accordance with this, TNF-α and IFN-γ inducible protein 10 (IP-10/CXCL10) were strongly up-regulated during disease. Of the Th2 cytokines analyzed (IL-4, IL-5, and IL-13), only IL-5 was at measurable levels. This cytokine may support B cell proliferation, differentiation, and antibody secretion (12). The levels of the regulatory cytokine IL-10 and of the T reg cell transcription factor FoxP3 paralleled the observed expression of CD4 in diseased mice. Interestingly, we found no major differences between immunized WT SJL/J mice and TCR^{1640} mice, which suffered from classical paralytic EAE. In line with their clinical picture, ataxic mice showed higher expression levels of the analyzed genes in brain (which also includes cerebellum and brain stem) than did paralytic relapsed mice. Conversely, expression in spinal cord was higher in paralytic relapsed mice than in ataxic mice. Intriguingly, most analyzed factors were elevated even in healthy TCR^{1640} mice (score 0) as compared with healthy nontransgenic littermate (NTL) mice, likely indicating subclinical inflammation. Finally, during the remission phase, expression of all analyzed genes dropped down to similar values as in score 0–TCR^{1640} mice (Fig. S4).

Expansion of MOG-specific B cells in TCR^{1640} single-transgenic SJL/J mice

Single-transgenic TCR^{1640} mice showed evidence of a strong MOG-specific B cell response. Spontaneous EAE lesions of single-transgenic TCR^{1640} animals displayed prominent deposits of Ig and some activated complement (Fig. 4). Furthermore, the inflamed CNS tissue contained, besides $CD4^+$ and $CD8^+$ lymphocytes, substantial numbers of B cells (5–40% of infiltrated lymphocytes) expressing CD19 or B220 as revealed by immunocytochemistry and flow cytometry (Fig. 3 and Fig. 4 E).

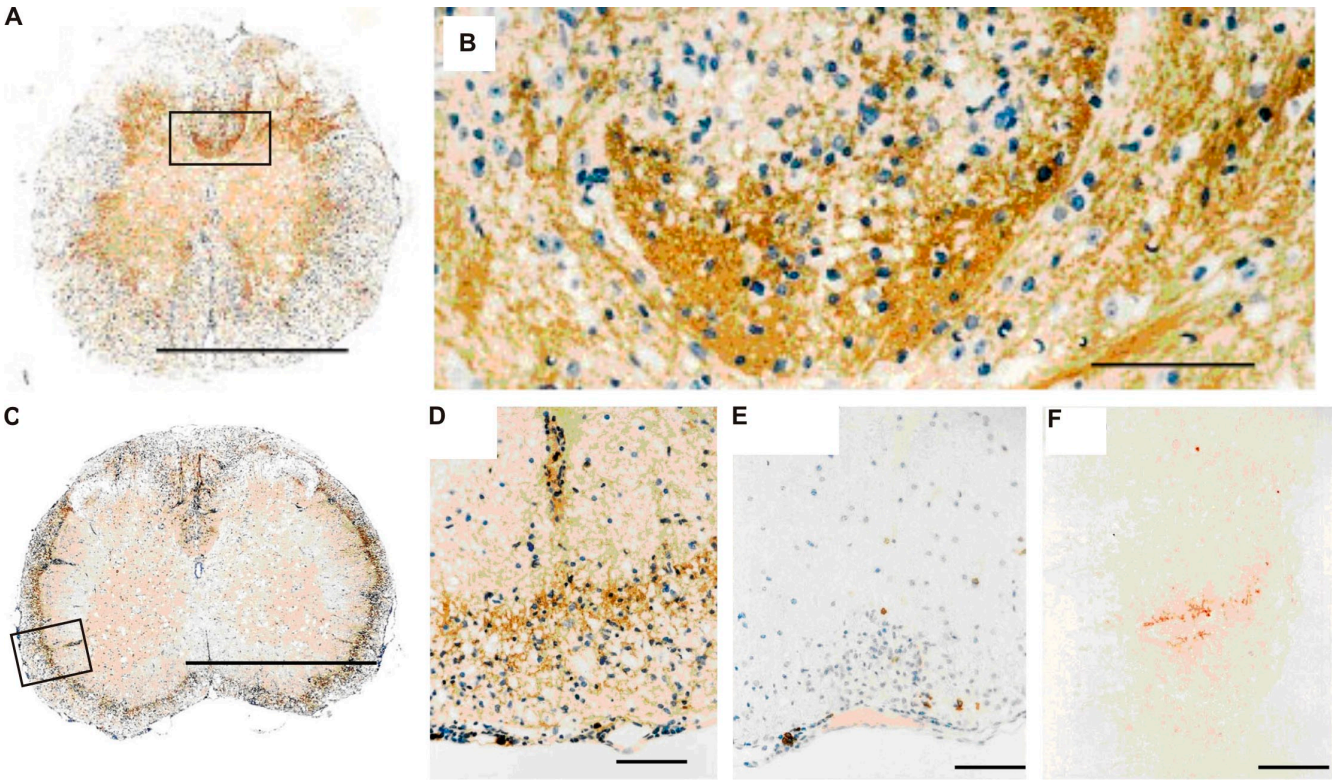

Figure 4. Ig deposition and B cell infiltrates in spinal cord of sick TCR^{1640} × IgH^{MOG} and TCR^{1640} mice. (A–D) Histological analysis of spinal cord using anti-Ig antibodies shows deposition of Ig in sick TCR^{1640} × IgH^{MOG} (A and B) and TCR^{1640} (C and D) mice (B and D show magnifications of marked areas in A and C, respectively). (E) Anti-B220 staining revealed some B cells among cellular infiltrates in sick TCR^{1640} mice. (F) Deposition of complement C9neo within CNS lesions of TCR^{1640} mice. Mononuclear cells were stained with H&E. Magnifications: A and C, ×50; B, ×425; D and E, ×200; F, ×450. Bars: (A and C) 1 mm; (B and D–F) 100 µm. Data are representative of at least two independent experiments consisting of more than three mice per group.

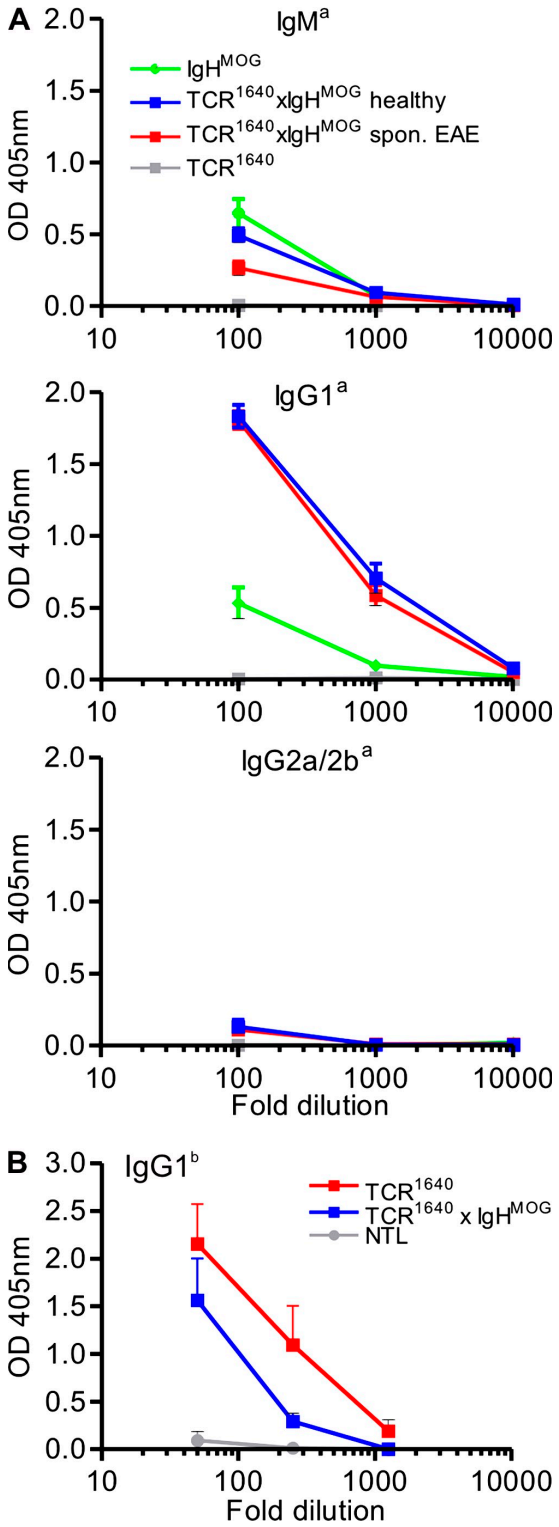

Figure 5. MOG-specific antibodies in double-transgenic TCR^{1640} × IgH^{MOG} and single TCR transgenic mice. (A) MOG binding allotype *a* autoantibodies were detected by ELISA in sera of indicated groups (each five to six mice). (B) Spontaneous anti-MOG IgG1 allotype *b* antibodies in TCR^{1640} and TCR^{1640} × IgH^{MOG} but not in NTL (n = 5 for each group). Sera at the indicated dilutions were incubated with plates precoated with rMOG. Bound anti-MOG Ig was detected by allotype-specific antibodies as indicated. Mean absorbance at OD 405 nm is shown. Error bars indicate SEM. Data are representative of two to three independent experiments.

Double-transgenic TCR^{1640} × IgH^{MOG} animals showed an anti-MOG antibody response dominated by the transgene-specific allotype *Igh^a*. In addition, however, a minor part of the MOG-specific antibodies expressed the endogenous nontransgenic *Igh^b* allotype (Fig. 5 B). Both antibody species were switched from IgM to IgG1 (Fig. 5, A and B).

Single-transgenic TCR^{1640} mice also produced anti-MOG autoantibodies (of endogenous *Igh^b*-allotype) reaching titers similar to those from WT mice immunized with rMOG (Fig. 6 A). The anti-MOG Igs were mainly of IgG1 and IgG2a/b isotypes, with very little IgM. The spontaneously appearing anti-MOG transgenic high frequency TCR^{1640} mice formed autoantibodies irrespective of their EAE status. This contrasted with low frequency single-transgenic TCR^{1586}, where anti-MOG autoantibodies were noted solely in the few animals with spontaneous EAE but not in resistant mice (Fig. 6 B). Also, mice of the EAE-resistant medium frequency line TCR^{1639} did not produce spontaneous MOG-specific antibodies. Development of spontaneous MOG antibodies was dependent on the presence of the autoantigen. Sera of MOG-deficient TCR^{1640} mice (bred on the *Mog*-deficient [*Mog*$^{-/-}$] background [reference 13]) did not contain any MOG-specific antibodies (Fig. 6 B). The B cell response in TCR^{1640} mice was specific to MOG and did not extend to other autoantigens (Fig. 6 C). In single-transgenic TCR^{1640} mice, autoantibodies became demonstrable from 5 wk of life and, in our series of measurements, persisted up to 9–10 wk, but very young mice, up to 4 wk of age, had no anti-MOG Igs (IgG1 and IgG2a/b isotypes) (Fig. 6 D).

Contribution of endogenous B cells and anti-MOG autoantibodies to RR spontaneous EAE

There is evidence that only autoantibodies directed against conformational epitopes, not linear epitopes, are involved in the pathogenesis of EAE (14) and that SJL/J mice, but not C57BL/6 mice, are able to produce such antibodies upon immunization with rMOG in CFA (15). The anti-MOG autoantibodies formed spontaneously in TCR^{1640} mice also bound to correctly folded MOG expressed on the surface of transduced EL4 cells and, thus, behaved like the classical anticonformational MOG mAb 8.18-C5 and its H chain transgene in TCR^{1640} × IgH^{MOG} mice (16) (Fig. 7 A). Binding of autoantibodies from TCR^{1640} and sick TCR^{1586} mice to EL4-MOG cells (dilutions of 1:20 and 1:200) followed by rabbit complement (Fig. 7 B) resulted in the specific lysis of the target cells. Sera from healthy TCR^{1586} and TCR^{1639} or *Mog*-deficient TCR^{1640} did not support lysis (unpublished data).

We confirmed the pathogenic potential of antibodies, in vivo. We immunized WT SJL/J mice with a low dose of PLP 139–151 and with incipient clinical EAE symptoms (between scores 0.5 and 1), we transferred serum either from TCR^{1640} mice (high titers of anti-MOG antibodies documented by ELISA) or NTLs, and compared the effects with the standard

anti-MOG monoclonal antibody 8.18C-5. In mice that had received TCR^{1640} serum, we noted a statistically significant increase in EAE severity similar to that of 8.18C-5 mAb (Fig. 8 A).

To examine the importance of B cells in the development of spontaneous EAE, we depleted B cells in TCR^{1640} mice using a monoclonal mouse anti–mouse CD20 antibody. TCR^{1640} mice were treated with anti-CD20 or isotype control (mouse IgG2a) every 2 wk starting on day 3. This protocol removed the B cells from peripheral blood, as well as spleen and lymph nodes, but left significant numbers of B cells in the bone marrow (Fig. S5, A and B). B cell depletion went along with either complete or partial loss of anti-MOG IgG1

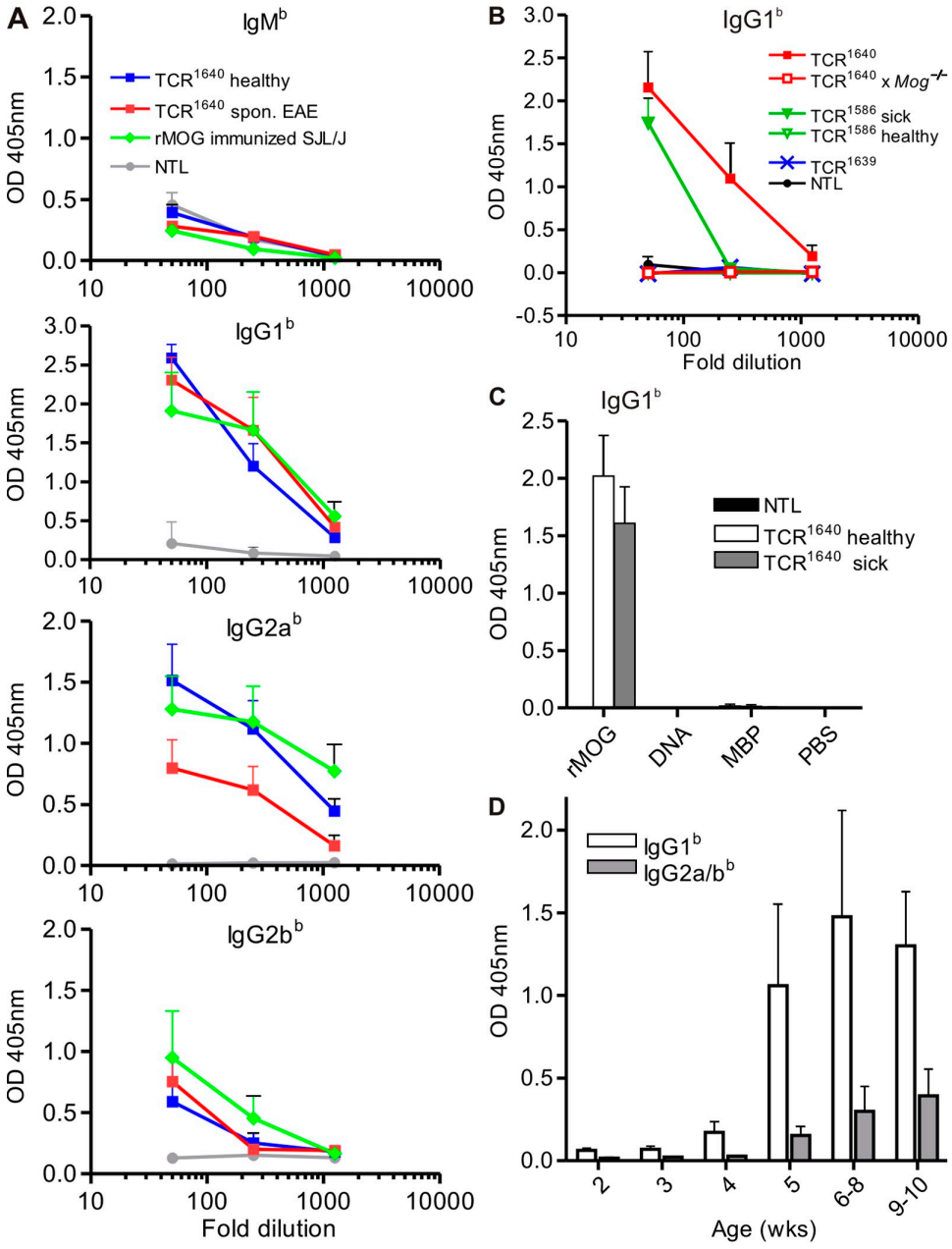

Figure 6. MOG-specific antibodies in single TCR transgenic mice. (A) Endogenous MOG binding antibodies of allotype *b* were measured by ELISA in sera of NTLs, healthy and sick TCR^{1640}, and rMOG-immunized WT SJL/J ($n = 6$ for each group). (B) Anti-MOG Igs of IgG1^b isotype are formed in TCR^{1640} and sick TCR^{1586} but not in TCR^{1639} or TCR^{1586} mice. Control NTLs, as well as TCR^{1640} mice deficient for MOG (*Mog*$^{-/-}$), are devoid of MOG binding autoantibodies (each three to five mice per group). (C) Autoantibodies in sera from TCR^{1640} mice are specific for MOG. Anti-MOG Ig antibodies, but not anti-MBP or anti–DNA-specific antibodies, were detected by ELISA in sera from TCR^{1640} mice (1/50 diluted) using IgG1^b-specific antibodies ($n = 5$). (D) Appearance of anti-MOG IgG1^b and IgG2a/b^b in TCR^{1640} mice by 5 wk of age. MOG binding antibodies were measured in 1/100 diluted sera from mice of different ages, each with three to five mice per group. Sera at the indicated dilutions were incubated with plates precoated with rMOG. Bound anti-MOG Ig was detected by allotype-specific antibodies as indicated. Mean absorbance at OD 405 nm is shown. Error bars indicate SEM. Data are representative of two independent experiments.

serum autoantibodies (Fig. S5 C). Within an observation period of up to 30 wk, only one out of nine anti-CD20–treated mice presented mild and transient EAE symptoms, whereas in mice receiving control antibody, spontaneous EAE was noted in >85% of the cases (Fig. 8 B and Table S3).

DISCUSSION

The RR mouse, as described in this paper, is the first transgenic mouse model that recapitulates the major features of RR-MS, the most prevalent type of human inflammatory demyelination. The disease starts spontaneously and, in contrast to OSE mice described previously (2, 3), in most cases takes an RR course, with clinical signs differing between individual bouts. Importantly, development of spontaneous disease goes along with the expansion of myelin autoimmune B cells from the endogenous immune repertoire.

Spontaneous RR-EAE

RR mice are transgenic SJL/J mice expressing at high frequency a TCR specific for MOG peptide 92–106 in the context of I-A^s. RR mice differ substantially from previously created transgenic SJL/J mice expressing TCRs recognizing a dominant peptide of PLP (17). These animals, kept under specific pathogen-free conditions, developed spontaneous disease but, in contrast to RR mice, the disease was mostly progressive without remissions and subsequent relapses.

The course and clinical expression of autoimmune diseases are determined by diverse factors, both genetic and environmental. Indeed, SJL/J mice are predisposed to develop fluctuating disease. Depending on the protocol applied, active immunization against encephalitogenic proteins may trigger RR disease (18). Clearly, this response pattern is facilitated by distinct regulatory genes (19), which may also influence spontaneous EAE developing in RR mice. So far, our breeding results suggest that B10.S mice, which have a distinct genetic background but share the MHC and the TCR transgene with SJL/J RR mice, very rarely develop spontaneous EAE, and in the few cases observed, the disease took a chronic rather than RR course (unpublished data).

Most variants of induced EAE present a stereotypical clinical syndrome with motor deficiencies starting at tail and hind limbs and progressing cranially with ongoing disease. Histologically, this clinical picture is reflected by a caudocranial gradient of inflammatory lesions (20). In a few models, however, additional parts of the CNS are affected. For example, in C57BL/6 mice, MOG-induced EAE has a predilection to affect the optic nerve (2, 3), and cerebellar disease was noted in further antigen/mouse combinations (21, 22). Our RR mouse models are the first to show immune attacks against different CNS parts in subsequent inflammatory relapses. They thus provide a unique paradigm to study the mechanisms underlying the targeting of MS lesions within the CNS during ongoing disease.

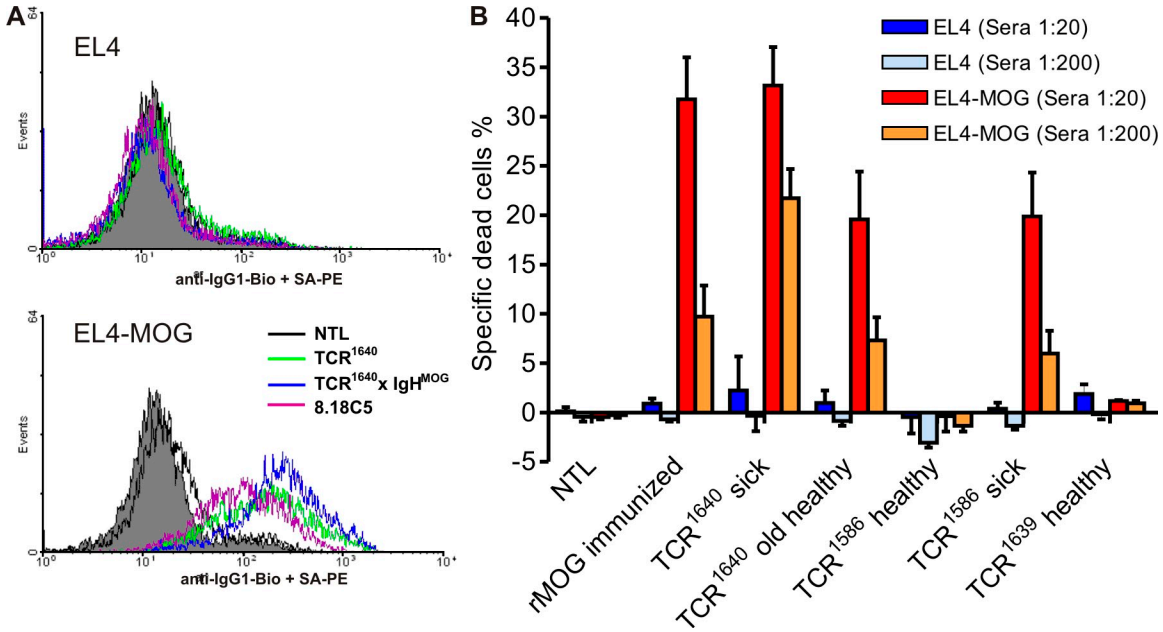

Figure 7. MOG-specific autoantibodies bind MOG-expressing cells and activate complement. (A) Binding of anti-MOG Ig from indicated mice to correctly conformed MOG on the cell surface of transduced EL4 cells (EL4-MOG) shown by flow cytometry. EL4 cells (top) and MOG-expressing EL4-MOG cells (bottom) were incubated with 1/200 diluted sera obtained from the indicated mice or 0.5 µg/ml 8.18-C5 mAb. Bound antibodies were detected by FACS using biotinylated anti–IgG1-specific antibody (allotype unspecific) and streptavidin-PE (SA-PE). A representative plot of three independent experiments is shown. (B) Complement activating capability of MOG binding antibodies in sera from transgenic mice. EL4 and EL4-MOG cells were incubated with sera (1/20 and 1/200 diluted) obtained from the indicated mice, each with three to five per group. Complement activating capability was measured by cell lysis using propidium iodide (PI) staining after incubation of sera-bound EL4 cells with rabbit complement. Background values were subtracted, and shown are mean values with the SEM of one experiment representative of three similar experiments.

Several investigators reported that in RR-EAE actively induced by immunization with encephalitogenic peptides, relapses went along with the T cell reactivity against new epitopes (23), a phenomenon termed "determinant spreading" by Lehmann et al. (24). Recent work by McMahon et al. (25) suggests that in actively induced chronic EAE, initial bouts of CNS inflammation result in the induction of professional APCs within or near the affected CNS target tissue. By taking up myelin antigens and presenting crucial epitope components to newly arrived naive autoreactive T cells, the repertoire of target autoantigens spreads (25). It should, however, be mentioned that determinant spreading, i.e., recruitment of potentially encephalitogenic T cells specific for epitopes other than MOG p92-106, has not been patent in spontaneous disease of our RR mice.

Expansion of MOG-specific B cells from endogenous repertoire

As described recently, in the C57BL/6 OSE model, MOG-reactive TCR transgenic T cells require the presence of MOG-specific B cells to kindle spontaneous EAE at high frequency. In this model, the MOG-specific B cells were transgenic with their germline IgJ region replaced by the rearranged H chain of a MOG-specific mAb (2, 3).

Based on these previous observations, we initially created double-transgenic mice by crossing our new MOG TCR

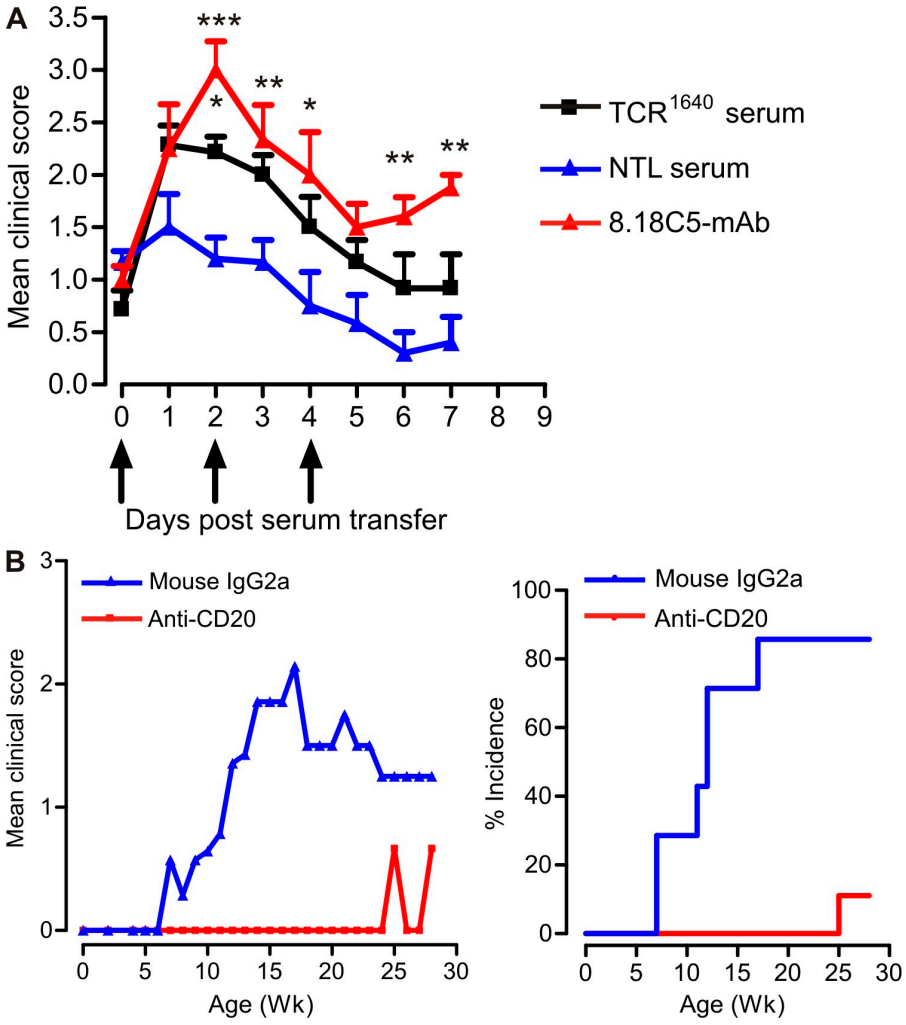

Figure 8. B cells and anti-MOG antibodies are essential for spontaneous EAE. (A) Spontaneously developed MOG-specific autoantibodies from TCR^{1640} mice have pathogenic potential. EAE was induced in WT SJL/J mice by low-dose PLP 139–151 immunization. Serum from TCR^{1640} mice, NTL mice, or 8.18c5 mAb were transferred after mice showed first clinical symptoms. Serum from TCR^{1640} mice significantly increased disease severity in recipient mice compared with serum from NTL mice. Error bars indicate SEM. *, $P < 0.05$; **, $P < 0.01$; ***, $P < 0.001$. Data were pooled from two independent experiments, each six to seven per group. (B) B cell depletion protects TCR^{1640} mice from spontaneous EAE. B cells were depleted from TCR^{1640} mice by twice weekly injections of anti-CD20 antibodies from day 3 after birth, and control mice received mouse IgG2a antibodies. The development of spontaneous EAE was monitored regularly. Although 85% of isotype control antibody-treated mice developed spontaneous EAE, treatment with CD20 antibody protected TCR^{1640} mice from disease development. Shown are the disease course (left) and the spontaneous EAE incidence (right) of TCR^{1640} mice treated with these antibodies. Data were pooled from two independent experiments, each with six to seven per group.

transgenic SJL/J strain with MOG-specific B cell knock-in SJL/J mice. These mice presented with spontaneous RR-EAE at high frequency. Less expected spontaneous EAE was noted also in TCR single-transgenic SJL/J mice with a high proportion of MOG-reactive CD4 T cells but without transgenic B cells. It turned out that in these TCR single-transgenic mice, MOG-specific B cells were expanded from the endogenous B cell compartment. Substantial numbers of B cells were observed to invade the inflammatory lesions, and there were heavy local deposits of Ig along with some activated complement. Most importantly, TCR single transgenics produced high titers of anti-MOG autoantibodies of IgG1 and IgG2 isotypes, which bound to correctly conformed membrane bound autoantigen, destroyed MOG-expressing target cells, and, thus, have demyelinating potential (16).

MOG-reactive B cells are essential for the spontaneous development of RR-EAE. Depletion of B cells by treatment with anti-CD20 mAb profoundly suppressed RR-EAE when started at young age. Treatment of adult mice produced much more inconsistent results, a phenomenon which was recently noted in other investigations in actively induced EAE (26).

B cells contribute to immune and autoimmune responses by secreting humoral antibodies, by acting as APCs, and by releasing cytokines. RR mice, both single and double transgenic, produce MOG-specific autoantibodies that share their dominant isotype, IgG1, with the original demyelinating anti-MOG mAb 8.18-C5 and that, in vivo, aggravate EAE when transferred i.v. (27). Importantly, we found large Ig deposits in the demyelinating lesions of single- and double-transgenic RR mice. At least part of these antibodies may have been produced by local infiltrating B cells. In fact, B cells isolated from CNS infiltrates were found to secrete anti-MOG antibodies at high levels.

Beyond autoantibody secretion, MOG-specific B cells profoundly influence autoimmune responses by directly interacting with autoimmune T cells. In OSE mice, as well as in $TCR^{1640} \times IgH^{MOG}$ mice (unpublished data), MOG-specific B cells concentrate highly diluted MOG and present the antigen to MOG-reactive T cells. Hence, antigen-presenting B cells may contribute to the initiation and progression of spontaneous EAE. But, in addition, B cells may act into the opposite direction; they were shown to limit EAE by releasing IL-10 (28) and by influencing function of regulatory T cells (29).

The spontaneous recruitment and expansion of autoimmune B cells from the endogenous repertoire by organ-specific autoimmune T cells in the absence of exogenous autoantigen represents a mechanism of autoimmunity that has not yet been described. The MOG-specific B cell expansion process critically requires the presence of the endogenous target autoantigen, as *Mog*-deficient TCR transgenic SJL/J mice never produced anti-MOG autoantibodies, nor did they develop spontaneous RR-EAE.

The role of endogenous MOG is intriguing, considering that this target autoantigen is predominantly confined to the CNS tissues, which are largely inaccessible to circulating T and B cells. This hidden localization distinguishes the RR mouse paradigm from transgenic mice, where activation of virus-specific B cell was noted in the presence of high numbers of virus-specific transgenic $CD4^+$ T cells and a viral pseudo-autoantigen expressed throughout the organism in cell types including DCs and macrophages (30).

Several mechanisms could be involved in MOG-specific B cell expansion. MOG-specific T cells could intrude into the naive CNS and create immunogenic conditions that allow the activation and expansion of naive B cells in the local milieu. This scenario has been forwarded recently as an explanation of epitope spreading in actively induced EAE (25). Alternatively, immunogenic MOG and/or myelin debris could be transported to local lymph nodes, either as cell-free material or by phagocytes, to be presented there to autoreactive B cells (31). Although MOG is predominantly expressed in the CNS, its messenger RNA was also found in some non-CNS organs, such as thymus, spleen, and liver (13, 32, 33), and low protein levels were found in the peripheral nervous system (34). Presentation of very low amounts of peripherally available MOG remains, at least in theory, an alternative mechanism of B cell expansion in RR mice.

Finally, animal models with spontaneously developing EAE show promise for the discovery of new drugs and the validation of existing medications. Thus, the opticospinal type of EAE described previously may represent essential features of human OSMS/Devic's disease (2), a disease variant which is rarely found in high prevalence populations. The spontaneous RR-EAE, with its conspicuous variation of neurological deficiencies, will provide a model for the most frequent type of MS, as it is seen typically in early phases of the disease.

MATERIALS AND METHODS

Mice. SJL/J mice were purchased from Charles River Laboratories. *Mog* KO mice (13) were backcrossed into SJL/J for seven generations, crossed with TCR^{1640} transgenic SJL/J mice, and then intercrossed to generate TCR^{1640} transgenic *Mog* KO mice. All mouse strains were bred in the animal facilities of the Max Planck Institute of Neurobiology (Martinsried, Germany).

Generation of TCR transgenic mice. TCR donor clone (C3) was selected from a panel of MOG-specific T cell clones (series SL48) derived from a SJL/J mouse immunized with rMOG in CFA. The encephalitogenic clone C3 uses Vα8.3 along with Vβ4 and recognizes $MOG_{92\text{-}106}$ bound to $I\text{-}A^s$. Total RNA of clone C3 was isolated by TRI reagent extraction (Sigma-Aldrich) and, after DNase I treatment, was converted into complementary DNA (cDNA) using hexanucleotide primers and Superscript II reverse transcription (Invitrogen). The rearranged cDNA of TCR-α8.3 and TCR-β4 chains were amplified with the following primer pairs: TCR-α8.3 sense with SalI restriction site, 5′-AGGTGTCGACCTTCCATGAACAT-GCGTCCTGACACC-3′; TCR-α C terminus with BamHI restriction site, 5′-ATAGGATCCTCAACTGGACCACAGCCTCAGC-3′; TCR-β4 sense with SalI restriction site, 5′-AGGTGTCGACTGACACTGCTATGG-GCTCCATTTTCCTC-3′; and TCR-β C2 terminus with BamHI restriction site, 5′-ATAGGATCCGGGTGAAGAACGGCTCAGGATGC-3′ (all synthesized at Metabion). The rearranged TCR-α8.3 and TCR-β4 chains from C3 cDNA were verified by sequencing. To eliminate a XhoI restriction site (CTC GAG) in TCR-β4 at aa 116, GAG was changed into GAA, both coding for glutamate, using a site-directed mutagenesis kit (Agilent Technologies) with the following primer pair: Vβ4 XhoI–Mut sense, 5′-CCAGA-CTGACTGTTCTCGAAGATCTGAGAAATGTG-3′; and Vβ4 XhoI–Mut, 5′-CACATTTCTCAGATCTTCGAGAACAGTCAGCTGG-3′. The amino acid sequence of the CDR3 regions is as follows: TCα8.3, LYY

CALSGGNNAPR FG (V8.3J4); and TCR-β4, CASS QERT DSAE TLY (V4D1J2.3C2). The complete rearranged TCR chains were cloned into the pHSE3′ vector (35), leading to expression under the control of the transgenic MHC class I H2-K^b promoter. XhoI-linearized TCR-containing plasmids were coinjected into the pronuclei of fertilized FVB oocytes. Transgenic founders were identified by PCR using a specific primer for C3 Vα-Jα or Vβ-Jβ in combination with a pHSE3′-specific primer (TCR-α chain: mTCR-Vα8.3-CDR3 sense, 5′-CTCCATAAGAGCAGCAGCTCC-3′, and hu β-globin antisense, 5′-CGTCTGTTTCCCATTCTAAACTGTACC-3′; TCR-β chain: PH-2Kb sense, 5′-CTGGATATAAAGTCCACGCAGCC-3′, and TCR-Vβ4-CDR3 antisense, 5′-CAATCTCTGCTTTTGATGGCTCAAAC-3′). Transgenic mice were backcrossed for at least eight generations into the SJL/J background.

EAE induction and scoring. Mice were injected s.c. at the back with 200 μl of recombinant MOG (200 μg), which was emulsified in Freund's adjuvant and supplemented with 3 mg/ml *Mycobacterium tuberculosis* (strain H37Ra). 200 ng of pertussis toxin was injected i.p. on days 0 and 2 after immunization. Clinical scoring of classical paralytic EAE was performed as follows: score 0, healthy; 1, flaccid tail; 1.5, flaccid tail and impaired righting reflex; 2, impaired righting reflex and hind limb weakness; 2.5, one hind leg paralyzed; 3, both hind legs paralyzed with residual mobility in both legs; 3.5, both hind legs completely paralyzed; 4, both hind legs completely paralyzed and beginning front limb paralysis; and 5, moribund or death of the animal after preceding clinical disease. Ataxic scoring was as follows: score 0, healthy; 1, mouse partly tilted, feet fall into cage fence; 2, tilted and tumbles; 3, mouse heavily tilted and moves in circles; 4, inability to walk, is only rolling. and 5, moribund. All animal procedures used were in accordance with guidelines of the committee on animals of the Max Planck Institute of Neurobiology and with the license of the Regierung von Oberbayern (Munich, Germany).

Antigens. Recombinant histidine-tagged rat MOG protein (aa 1–125) was purified from bacterial inclusion bodies (36). MOG peptide 90–110 (SDEGGYTCFFRDHSYQEEAA), MOG 1–26 (GQFRVIGPGYPIRALVGDEAELPCRI), and MOG 92–106 (DEGGYTCFFRDHSYQ) were synthesized at the core facility of the Max Planck Institute of Biochemistry (Martinsried, Germany) or BioTrend (Köln, Germany). All antigens used in the study were of >95% purity, analyzed by silver staining of PAGE (proteins) or HPLC analysis (peptides).

In vitro proliferation assay. Proliferation assays were performed as previously described (2). Each sample was run in triplicates, the proliferative response of which is represented by the mean ± SEM. All assays were replicated at least three times.

ELISA. Cytokine measurements and determination of serum titers of MOG-specific antibodies was performed as previously described (2). Antibodies were obtained from BD, except the anti–IL-17 which was obtained from R&D Systems. Each assay was repeated at least three times.

Flow cytometric analysis. Single cell suspensions were prepared from spleen, lymph node, thymus, or CNS tissue by mechanical disruption via forcing trough 40-μm cell strainers (BD). Erythrocytes of spleen cell suspensions were lysed by hypotonic treatment. CNS infiltrate cells were purified by Percoll gradient centrifugation. Cells were resuspended in Percoll (GE Healthcare) at a density of 1.035 g/ml and centrifuged over Percoll of a 1.08-g/ml density for 30 min at 20°C. The interphase was recovered and subjected to FACS analysis. For detection of cell surface markers by flow cytometric analysis, cells were stained in FACS medium (PBS containing 1% BSA and 0.1% NaN_3) with different fluorochrome-labeled MAbs. For cytofluorometry, we used the FACSCalibur system with CellQuest software (BD), and for analysis we used WinMDI 2.9 software (Joe Trotter, The Scripps Institute, La Jolla, CA) was used. For intracellular cytokine staining, cells were first surface stained and then fixed and permeabilized in 4% PFA/0.1% saponin in Hepes-buffered HBSS, stained intracellularly, and washed. Before staining, cells were activated with 50 ng/ml PMA/500 ng/ml ionomycin in the presence of 5 μg/ml brefeldin A for 4 h. The following fluorochrome-labeled antibodies were purchased from BD or eBioscience: CD3 (145-2C11), CD4 (RM4-5), CD8 (53–6.7), Vα8.3 (B21.14), Vβ4 (KT4), CD11b (M1/70), CD45.1 (A20), CD19 (1D3), B220 (RA3-6B2), CD62L (MEL-14), CD25 (PC61), IFN-γ (XMG1.2), IL-17 (TC11-18H10), and IgG1 (A85-1).

Histological analysis. Brain and spinal cord tissue from mice fixed by perfusion with 4% phosphate buffered paraformaldehyde were embedded in paraffin. Paraffin sections were stained with H&E, with Luxol fast blue for myelin, and by Bielschowsky silver impregnation for visualization of neurons and axons. Adjacent serial sections were stained by immunocytochemistry, using primary antibodies directed against CD3, B220, Mac-3, mouse Ig, and rat/mouse complement C9 neoantigen. Immunocytochemistry was performed with a biotin avidin technique.

Quantitative real-time TaqMan PCR analysis. Real time quantitative PCR analysis was performed as previously described (2). Quantification of the expression of mouse immune and housekeeping genes was performed by Taqman PCR using the following primer/probe combinations: GAPDH sense, 5′-TCACCACCATGGAGAAGGC-3′; GAPDH antisense, 5′-GCTAAGCAGTTGGTGGTGCA-3′; GAPDH probe, 5′-ATGCCCCCATGTTTGTGATGGGTGT-3′; mIL-5 sense, 5′-CCGCTCACCGAGCTCTGTT-3′; mIL-5 antisense, 5′-AGATTTCTCCAATGCATAGCTGG-3′; IL-5 probe, 5′-CAGGAAGCCTCATCGTCTCATTGCTTGT-3′; mIL-10 sense, 5′-CAGAGAAGCATGGCCCAGAA-3′; mIL-10 antisense, 5′-TGCTCCACTGCCTTGCTCTT-3′; mIL-10 probe, 5′-TGAGGCGCTGTCATCGATTTCTCCC-3′; mIL-17 sense, 5′-AACTCCCTTGGCGCAAAAGT-3′; mIL-17 antisense, 5′-GGCACTGAGCTTCCCAGATC-3′; mIL-17 probe, 5′-CCACGTCACCCTGGACTCTCCACC-3′; mCD4 sense, 5′-CGTTTCCTCTCATCATCAATAAACTTA-3′; mCD4 antisense, 5′-GGCTGGTACCCGGACTGAAG-3′; mCD4 probe, 5′-CACTTTGAACACCCACAACTCCACCTCCT-3′; TCR-Vα8.3 sense, 5′-CCACGCCACTCTCCATAAGAG-3′; TCR-Vα8.3 antisense, 5′-CAGTAGTACAGGCCAGAGTCTGACA-3′; TCR-Vα8.3 probe, 5′-CCTGAGCCAAAATACAGCGTTT-3′; TCR-Vβ sense, 5′-TGATGACTCGGCCACATACTTC-3′; TCR-Vβ4 antisense, 5′-AGCAGCTCCTTCCATCTGCAGAAGTCC-3′; TCR-Vβ4 probe, 5′-TGCCAGCAGCCAAGAACGGACAGAT-3′; mFoxP3 sense, 5′-AGGAGAAGCTGGGAGCTATGC-3′; mFoxP3 antisense, 5′-TGGCTACGATGCAGCAAGAG-3′; and mFoxP3 probe, 5′-AAGGCTCCATCTGTGGCCTCAATGGA-3′. IFN-γ, TNF-α, IL-4, IL-13, and IP-10 Taqman probes were synthesized as described in Giulietti et al. (37).

Cell surface serum binding and complement assay. For EL4-MOG cells, the mouse *Mog* cDNA was cloned into the retroviral vector pLXSN (Clontech Laboratories, Inc.) and transformed into a GP^+E-86 packaging cell line. Virus-containing supernatant was used to stably transduce the mouse EL4 lymphoma cell line. EL4 and MOG-transduced EL4 cells (EL4-MOG; 2×10^5/well) were incubated with sera at the indicated dilutions for 30–45 min at 4°C, washed intensively, and thereafter either stained with biotinylated anti–mouse IgG1 (BD) and streptavidin–PE diluted at 1/150 and PI at 1 μg/ml or incubated with LOW-TOX-M rabbit complement (Cedarlane Laboratories) at a 1/10 dilution for 90 min at 37°C and thereafter analyzed for lysis by staining with PI. For analysis of binding only live (PI^-) cells are gated for the histograms.

Depletion of B cells. For B cell depletion, 20 μg of mouse anti–mouse CD20 (18B12; IgG2a; Biogen Idec) (38) or IgG2a control antibody (Sigma-Aldrich) was injected s.c. into 3-d-old TCR^{1640} mice. 2 wk later, pups were injected with 80 μg and, at 4 wk old, with 250 μg of respective antibodies. Injections were repeated thereafter at 2-wk intervals with 250 μg of respective antibodies.

Serum transfer. Sera were obtained through retroorbital bleeding from TCR^{1640} or NTL. WT SJL/J mice were immunized with 100 μg PLP139-151 in 5 mg/ml CFA. 200 ng of Pertussis toxin was injected on days 0 and 2. When mice showed clinical EAE signs (score ∼1.0), they received i.p. injections of 250 μl TCR^{1640} serum or NTL serum or 8.18c5 mAb three times at 48-h intervals.

Statistics. Differential spontaneous EAE incidence of female to males was analyzed by logrank test (by an in-built survival curve analysis function from Prism 4 [Graph Pad Software, Inc.]), and the effect of serum transfer on EAE development was analyzed by two-way ANOVA. P-values < 0.05 were considered to be significant.

Online supplemental material. Fig. S1 shows the nature and encephalitogenicity of TCR donor clone C3. Fig. S2 shows the TCR expression in TCR^{1640} transgenic mice splenocytes. Fig. S3 illustrates the spontaneous disease course of individual transgenic TCR^{1640} animals. Fig. S4 shows the CNS messenger RNA expression analysis of spontaneous EAE- and MOG-immunized mice. Fig. S5 shows the efficiency of B cell depletion in TCR^{1640} mice. Video S1 shows one diseased double-transgenic mouse in different EAE stages. Table S1 shows a summary of spontaneous EAE in TCR transgenic SJL/J mice. Table S2 shows a summary of histological analysis of representative individual mice with spontaneous EAE. Table S3 summarizes spontaneous EAE incidence and mortality in TCR^{1640} mice treated with anti-CD20 and control isotype antibodies. Online supplemental material is available at http://www.jem.org/cgi/content/full/jem.20090299/DC1.

We are grateful to Irene Arnold-Ammer, Lydia Penner, Iris Jarsch, Michaela Krug, Marianne Leiszer, and Ulrike Köck for excellent technical support.

This project was supported by the Deutsche Forschungsgemeinschaft (SFB 571, Project B6) and the Max Planck society. S.H. Domingues is supported by a PhD fellowship (Portuguese FCT program SFRH/BD/15885/2005).

The authors have no conflicting financial interests.

Submitted: 6 February 2009
Accepted: 3 May 2009

REFERENCES

1. Krishnamoorthy, G., A. Holz, and H. Wekerle. 2007. Experimental models of spontaneous autoimmune disease in the central nervous system. *J. Mol. Med.* 85:1161–1173.
2. Krishnamoorthy, G., H. Lassmann, H. Wekerle, and A. Holz. 2006. Spontaneous opticospinal encephalomyelitis in a double-transgenic mouse model of autoimmune T cell/B cell cooperation. *J. Clin. Invest.* 116:2385–2392.
3. Bettelli, E., D. Baeten, A. Jäger, R.A. Sobel, and V.K. Kuchroo. 2006. Myelin oligodendrocyte glycoprotein-specific T and B cells cooperate to induce a Devic-like disease in mice. *J. Clin. Invest.* 116:2393–2402.
4. Kira, J. 2003. Multiple sclerosis in the Japanese population. *Lancet Neurol.* 2:117–127.
5. Compston, A. 2004. 'The marvellous harmony of the nervous parts': The origins of multiple sclerosis. *Clin. Med.* 4:346–354.
6. Litzenburger, T., R. Fässler, J. Bauer, H. Lassmann, C. Linington, H. Wekerle, and A. Iglesias. 1998. B lymphocytes producing demyelinating autoantibodies: development and function in gene-targeted transgenic mice. *J. Exp. Med.* 188:169–180.
7. Chen, Y., C.L. Langrish, B. McKenzie, B. Joyce-Shaikh, J.S. Stumhofer, T. McClanahan, W. Blumenschein, T. Churakova, J. Low, L. Presta, et al. 2006. Anti-IL-23 therapy inhibits multiple inflammatory pathways and ameliorates autoimmune encephalomyelitis. *J. Clin. Invest.* 116:1317–1326.
8. Veldhoen, M., R.J. Hocking, R.A. Flavell, and B. Stockinger. 2006. Signals mediated by transforming growth factor-β initiate autoimmune encephalomyelitis, but chronic inflammation is needed to sustain disease. *Nat. Immunol.* 7:1151–1156.
9. Bettelli, E., Y. Carrier, W. Gao, T. Korn, T.B. Strom, M. Oukka, H.L. Weiner, and V.K. Kuchroo. 2006. Reciprocal developmental pathways for the generation of pathogenic effector TH17 and regulatory T cells. *Nature.* 441:235–238.
10. Bailey, S.L., B. Schreiner, E.J. McMahon, and S.D. Miller. 2007. CNS myeloid DCs presenting endogenous myelin peptides 'preferentially' polarize $CD4^+$ TH-17 cells in relapsing EAE. *Nat. Immunol.* 8:172–180.
11. Hori, S., T. Nomura, and S. Sakaguchi. 2003. Control of regulatory T cell development by the transcription factor *Foxp3*. *Science.* 299:1057–1061.
12. Kishimoto, T., and T. Hirano. 1988. Molecular regulation of B lymphocyte response. *Annu. Rev. Immunol.* 6:485–512.
13. Delarasse, C., P. Daubas, L.T. Mars, C. Vizler, T. Litzenburger, A. Iglesias, J. Bauer, B. Della Gaspera, A. Schubart, L. Decker, et al. 2003. Myelin/oligodendrocyte glycoprotein-deficient (MOG-deficient) mice reveal lack of immune tolerance to MOG in wild-type mice. *J. Clin. Invest.* 112:544–553.
14. von Büdingen, H.C., S.L. Hauser, A. Fuhrmann, C.B. Nabavi, J.I. Lee, and C.P. Genain. 2002. Molecular characterization of antibody specificities against myelin/oligodendrocyte glycoprotein in autoimmune demyelination. *Proc. Natl. Acad. Sci. USA.* 99:8207–8212.
15. Bourquin, C., A. Schubart, S. Tobollik, I. Mather, S. Ogg, R. Liblau, and C. Linington. 2003. Selective unresponsiveness to conformational B cell epitopes of the myelin oligodendrocyte glycoprotein in $H\text{-}2^b$ mice. *J. Immunol.* 171:455–461.
16. Brehm, U., S.J. Piddlesden, M.V. Gardinier, and C. Linington. 1999. Epitope specificity of demyelinating monoclonal autoantibodies directed against the human myelin oligodendrocyte glycoprotein. *J. Neuroimmunol.* 97:9–15.
17. Waldner, H., M.J. Whitters, R.A. Sobel, M. Collins, and V.K. Kuchroo. 2000. Fulminant spontaneous autoimmunity of the central nervous system in mice transgenic for the myelin proteolipid protein-specific T cell receptor. *Proc. Natl. Acad. Sci. USA.* 97:3412–3417.
18. Moore, G.R., R.M. McCarron, D.E. McFarlin, and C.S. Raine. 1987. Chronic relapsing necrotizing encephalomyelitis produced by myelin basic protein. *Lab. Invest.* 57:157–167.
19. Butterfield, R.J., E.P. Blankenhorn, R.J. Roper, J.F. Zachary, R.W. Doerge, J.D. Sudweeks, J. Rose, and C. Teuscher. 1999. Genetic analysis of disease subtypes and sexual dimorphisms in mouse experimental allergic encephalomyelitis (EAE): Relapsing/remitting and monophasic remitting/nonrelapsing EAE are immunogenetically distinct. *J. Immunol.* 162:3096–3102.
20. Wekerle, H., and H. Lassmann. 2006. The immunology of inflammatory demyelinating disease. *In* McAlpine's Multiple Sclerosis. A. Compston, C. Confavreux, H. Lassmann, I. McDonald, D. Miller, J. Noseworthy, K. Smith, and H. Wekerle, editors. Churchill Livingstone, Oxford. 491-546.
21. Abromson-Leeman, S., R. Bronson, Y. Luo, M. Berman, R. Leeman, J. Leeman, and M. Dorf. 2004. T-cell properties determine disease site, clinical presentation, and cellular pathology of experimental autoimmune encephalomyelitis. *Am. J. Pathol.* 165:1519–1533.
22. Muller, D.M., M.P. Pender, and J.M. Greer. 2005. Blood-brain barrier disruption and lesion localization in experimental autoimmune encephalomyelitis with predominant cerebellar and brainstem involvement. *J. Neuroimmunol.* 160:162–169.
23. McCarron, R.M., R.J. Fallis, and D.E. McFarlin. 1990. Alterations in T cell antigen specificity and class II restriction during the course of chronic relapsing experimental allergic encephalomyelitis. *J. Neuroimmunol.* 29:73–79.
24. Lehmann, P.V., T. Forsthuber, A. Miller, and E.E. Sercarz. 1992. Spreading of T-cell autoimmunity to cryptic determinants of an autoantigen. *Nature.* 358:155–157.
25. McMahon, E.J., S.L. Bailey, C.L. Vanderlugt-Castaneda, H. Waldner, and S.D. Miller. 2005. Epitope spreading initiates in the CNS in two mouse models of multiple sclerosis. *Nat. Med.* 11:335–339.
26. Matsushita, T., K. Yanaba, J.-D. Bouaziz, M. Fujimoto, and T.F. Tedder. 2008. Regulatory B cells inhibit EAE initiation in mice while other B cells promote disease progression. *J. Clin. Invest.* 118:3420–3430.
27. Gunn, C., A.J. Suckling, and C. Linington. 1989. Identification of a common idiotype of myelin oligodendrocyte glycoprotein-specific autoantibodies in chronic relapsing experimental allergic encephalomyelitis. *J. Neuroimmunol.* 23:101–108.
28. Fillatreau, S., C.H. Sweenie, M.J. McGeachy, D. Gray, and S.M. Anderton. 2002. B cells regulate autoimmunity by provision of IL-10. *Nat. Immunol.* 3:944–950.
29. Mann, M.K., K. Maresz, L.P. Shriver, Y.P. Tan, and B.N. Dittel. 2007. B cell regulation of $CD4^+CD25^+$ T regulatory cells and IL-10 via B7 is essential for recovery from experimental autoimmune encephalomyelitis. *J. Immunol.* 178:3447–3456.

30. Guay, H.M., J. Larkin, C. Cozzo Picca, L. Panarey, and A.J. Caton. 2007. Spontaneous autoreactive memory B cell formation driven by a high frequency of autoreactive CD4$^+$ T cells. *J. Immunol.* 178:4793–4802.
31. De Vos, A.F., M. Van Meurs, H.P. Brok, L.A. Boven, R.Q. Hintzen, P. Van der Valk, R. Ravid, S. Rensing, L. Boon, B.A. 't Hart, and J.D. Laman. 2002. Transfer of central nervous system autoantigens and presentation in secondary lymphoid organs. *J. Immunol.* 169:5415–5423.
32. Derbinski, J., A. Schulte, B. Kyewski, and L. Klein. 2001. Promiscuous gene expression in medullary thymic epithelial cells mirrors the peripheral self. *Nat. Immunol.* 2:1032–1039.
33. Pagany, M., M. Jagodic, C. Bourquin, T. Olsson, and C. Linington. 2003. Genetic variation in myelin oligodendrocyte glycoprotein expression and susceptibility to experimental autoimmune encephalomyelitis. *J. Neuroimmunol.* 139:1–8.
34. Pagany, M., M. Jagodic, A. Schubart, D. Pham-Dinh, C. Bachelin, A.B. van Evercooren, F. Lachapelle, T. Olsson, and C. Linington. 2003. Myelin oligodendrocyte glycoprotein is expressed in the peripheral nervous system of rodents and primates. *Neurosci. Lett.* 350:165–168.
35. Pircher, H., T.W. Mak, R. Lang, W. Ballhausen, E. Rüedi, H. Hengartner, R.M. Zinkernagel, and K. Bürki. 1989. T cell tolerance to Mls^a encoded antigens in T cell receptor Vβ8.1 chain transgenic mice. *EMBO J.* 8:719–727.
36. Adelmann, M., J. Wood, I. Benzel, P. Fiori, H. Lassmann, J.-M. Matthieu, M.V. Gardinier, K. Dornmair, and C. Linington. 1995. The N-terminal domain of the myelin oligodendrocyte glycoprotein (MOG) induces acute demyelinating experimental autoimmune encephalomyelitis in the Lewis rat. *J. Neuroimmunol.* 63:17–27.
37. Giulietti, A., L. Overbergh, D. Valckx, B. Decallonee, R. Bouillon, and C. Mathieu. 2001. An overview of real-time quantitative PCR: Applications to quantify cytokine gene expression. *Methods.* 25:386–401.
38. Hamel, K., P. Doodes, Y.X. Cao, Y.M. Wang, J. Martinson, R. Dunn, M.R. Kehry, B. Farkas, and A. Finnegan. 2008. Suppression of proteoglycan-induced arthritis by anti-CD20 B cell depletion therapy is mediated by reduction in autoantibodies and CD4$^+$ T cell reactivity. *J. Immunol.* 180:4994–5003.